Mitochondrial Uptake of Sestamibi Distinguishes Between Normal, Inflammatory Breast Changes, Pre-Cancers, and Infiltrating Breast Cancer

Richard M. Fleming, MD, FICA, FACA, FASNC, FACP

The evaluation of breast tissue using nuclear imaging is dependent upon the delivery and uptake of the isotope by breast tissue. This is dependent upon blood flow to the breast and functioning mitochondria. This 2-part study investigated (1) differences in uptake of sestamibi when blood flow is enhanced (breast enhanced scintigraphy test [BEST]), and (2) differences in isotope uptake in normal (Nl) breast tissue, inflammatory changes in breast tissue (ICB), and breast cancer (CA). In the first part of the study, 10 women were compared using both Miraluma and BEST imaging; in the second part, 195 people were studied using BEST imaging only. The results were compared with histopathologic specimens. Little difference was noted between Miraluma and BEST imaging in the first part. Women with ICB showed a statistically significant ($P < .05$) increase in isotope uptake using BEST imaging. This difference was even more significant ($P < .005$) in women with CA. During the second part of the study, BEST imaging demonstrated an exponential increase in tracer uptake. When maximal count activity was compared, there was a statistically significant ($P < .001$) difference between Nl and ICB, between ICB and atypia (A), and between A and CA. BEST imaging demonstrated significant increases in isotope delivery when compared with Miraluma imaging. These differences allowed differentiation of breast tissue, including the detection of early changes in breast tissue.

The detection of breast cancer is based on finding an anatomic and/or a physiologic abnormality. Anatomic detection is made by breast self-examination by either the patient or the physician, mammography (radiographic detection), ultrasound evaluation of a lump/mass or mammographic abnormality, computed tomography (CT), or magnetic resonance imaging. Physiologic detection is made using either positron emission tomography (PET) imaging augmented by CT findings or single photon emission computed tomography (SPECT) imaging using sestamibi.

Sestamibi imaging has been shown to enhance the detection of breast cancers[1,2] and is a useful adjunct to mammography. The delivery and subsequent detection of sestamibi uptake by a tumor is dependent on (1) the delivery of the isotope to the cancer (blood flow) and (2) the presence of living tissue with active mitochondria. More than 90% of sestamibi is taken up by mitochondria[3] in an energy-dependent manner. This uptake increases with the number of mitochondria[4-6] present and the functional activity[7] of these mitochondria (i.e., the greater the activity of the cells, the greater the uptake of the mitochondria). Inflammatory cells[8] take up sestamibi to a greater extent than normal cells but to a lesser extent than cancer cells. This uptake demonstrates the ability of the cells to maintain a transmembrane potential[9,10] and has been used in cardiac imaging to demonstrate ischemic, infarcted, and viable[11-14] myocardium. As such, it has also been used to determine adriamycin-induced cardiotoxicity[15] following chemotherapy.

In addition to mitochondrial activity, the presence of sestamibi is dependent on its delivery to the region of the body being imaged, the delivery of which occurs through the bloodstream. Regions of inflammation and cancers, which produce angiogenic factors,[16-18] have greater vascularity, which can increase the delivery of sestamibi to tissues for imaging. Like breast cancer, the detection of coronary artery disease is also determined using anatomic (angiography, intravascular ultrasound) and/or physiologic (SPECT or PET imaging) methods. The ability to change coronary blood flow using high-dose dipyridamole (HDD) to detect coronary artery disease has been demonstrated.[19-24] This approach increases regional blood flow (coronary flow reserve) differences,[25,26] enhancing the detection of coronary artery disease, and as mentioned previously can simultaneously provide useful diagnostic information with regard to adriamycin cardiotoxicity. However, a prospective analysis of the results of combining breast imaging and cardiac imaging using HDD has not yet been made.

RMF is at the Camelot Foundation, Omaha, Nebraska.

Correspondence: Richard M. Fleming, Camelot Foundation, 9290 West Dodge Road, Suite 204, Omaha, NE 68114. E-mail: rfmd1@fhhi.omhcoxmail.com.

Based on the assumption that breast cancer should have increased vascularity, which could be influenced by the vasodilatory effect of dipyridamole (HDD), and greater mitochondrial activity, which could be further detected once increased delivery of sestamibi is provided through enhanced blood flow, this study was designed to determine whether such differences could be detected. During the first part of the study, we compared the results of 10 women studied using the resting (Miraluma) sestamibi imaging approach with results obtained following enhanced delivery of the isotope using HDD. In the second part of the study, 195 (4 men, 191 women) individuals were studied using the enhanced (HDD) approach only. The results of both parts were compared with biopsy data.

Methods

Subject Enrollment

Two hundred five individuals (201 women, 4 men) were studied during a 33-month period beginning in February 1999 and ending in November 2001. The individuals ranged in age from 27 to 88 years. During the first part of the study, all 10 women had either an abnormality on mammography or a detectable lump on physical examination. During the second part of the study, there were 4 men with detectable breast lumps and 191 women. Of the women, 58 were seeking additional information with regard to breast disease concerns and 133 had breast lumps and/or abnormal mammograms. Women were excluded from the study if they were taking hormone replacement therapy, were pregnant, or were breastfeeding. All subjects signed institutional consent forms prior to undergoing breast imaging.

Resting (Miraluma) Sestamibi Breast Imaging

Subjects undergoing breast imaging arrived at the Fleming Heart & Health Institute at the Camelot Foundation in the fasting state approximately 15 to 30 minutes prior to the study. A 20-gauge intravenous catheter was placed in the right arm, or in the left arm if the right breast was the breast in question. As shown in Figure 1, 25 to 30 mCi (925 to 1110 MBq) of technetium-99m hexakis 2-methoxyisobutylisonitrile (sestamibi) is administered intravenously at the 4-minute mark, with image acquisition beginning 6 minutes later. The patient is then placed in the prone position on top of a 6-inch foam pad designed to enhance the comfort of the patient while improving breast imaging. Each side of the 6-inch pad has breast inserts held in place by Velcro that can be removed to allow each breast to be positioned through the openings in a dependent manner without breast compression. Ten minutes into the study, image acquisition is started as shown in Figure 1. All images are acquired while the patient is prone, except for the anterior (BrAS) image, which is obtained while the patient is supine.

Breast image acquisition and reconstruction were performed using a Siemens orbiter SPECT camera with 75 photomultiplier tubes and a 128 by 128 matrix. The images are acquired with the camera head in a stationary (planar) position. The camera, computer, and software providing quantification of maximal count activity (MCA) were supplied by NC Systems (Boulder, CO). A low-energy, high-resolution collimator was used, which provided a resolution of 3.4 mm.

Images were displayed in a black-and-white format, as shown in Figure 2A. Regions of interest were then drawn around the entire breast and analysis was made for the greatest amount of tracer uptake. This greatest activity is the MCA and represents the region of breast tissue with the greatest blood flow and mitochondrial activity.

Breast Enhanced Scintigraphy (Sestamibi) Test Imaging

Subjects undergoing breast enhanced scintigraphy (sestamibi) test (BEST) imaging are prepared for the study in a manner identical to that used in the preparation for the resting (Miraluma) imaging. They arrive at the institute in a fasting state 15 to 30 minutes prior to the study, and a 20 gauge intravenous catheter is placed either in the right arm, or in the left arm if the right breast is the breast in question. As shown in Figure 1, enhancement of blood flow is provided by administering 0.852 mg of intravenous dipyridamole (HDD), infused over 4 minutes. Two minutes later, at peak dipyridamole effect, 25 to 30 mCi (925 to 1110 MBq) of technetium-99m hexakis 2-methoxyisobutylisonitrile (sestamibi) is administered intravenously. Image acquisition is started 10 minutes into the study, as shown in Figure 1, with the patient in a prone position. Anterior images are obtained with the patient in a supine position. Following breast imaging, cardiac imaging is performed as described previously,[20,25] providing information with regard to coronary blood flow, regional wall abnormalities, and left ventricular ejection fraction, which is useful for making further diagnostic decisions, particularly with regard to the use of chemotherapy and radiation therapy.

Breast imaging equipment and acquisition are identical to those used for the resting (Miraluma) image approach. The image display for BEST is displayed in a blue-green format to reduce artifacts reported previously.[27] An example of the blue-green format is shown in Figure 2A, juxtaposed with resting images. Figure 2B shows the sequence of processing

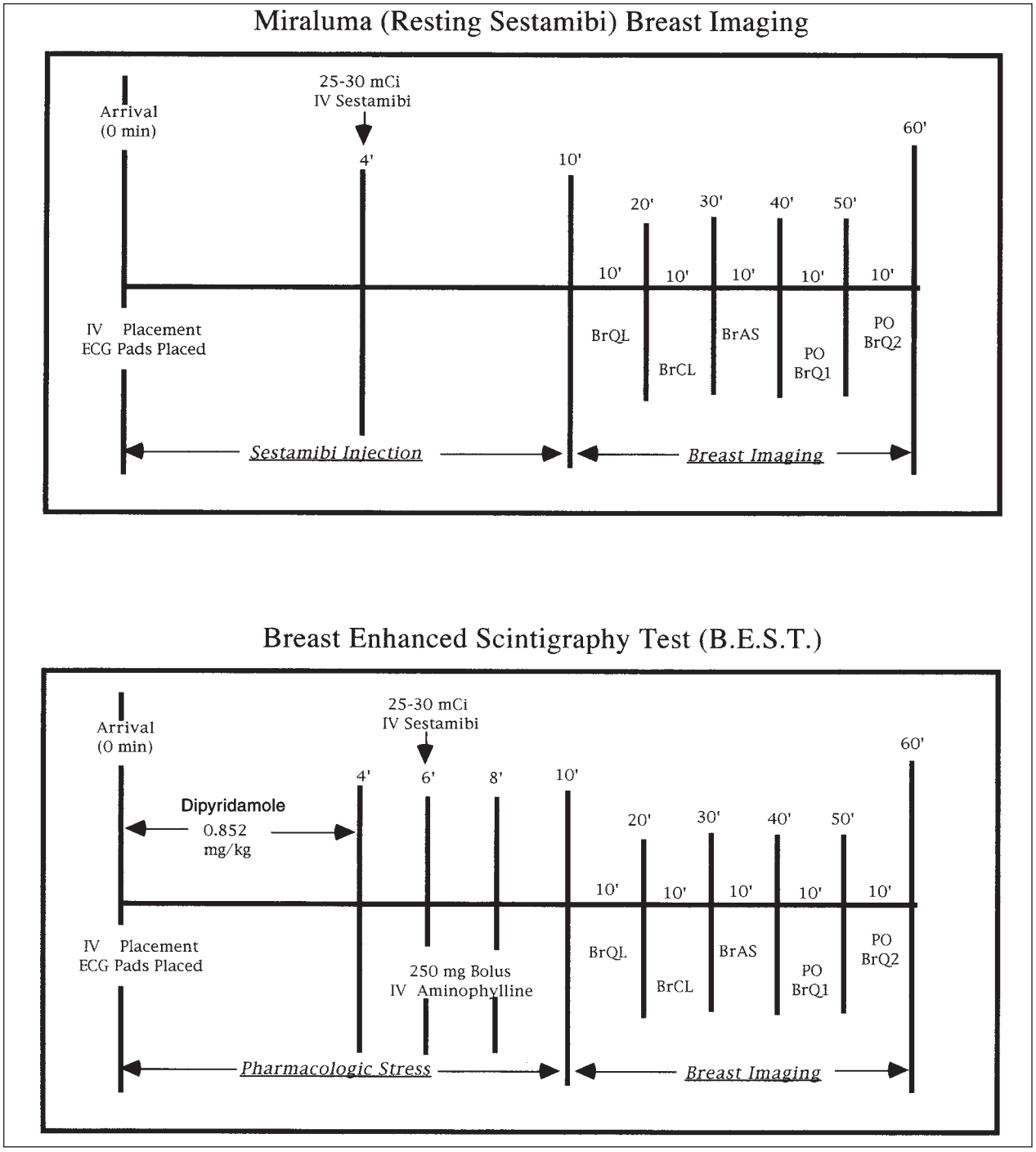

Figure 1 *Resting (Miraluma) and breast enhanced scintigraphy test (BEST) imaging protocols. The top panel displays the protocol for resting (Miraluma) imaging of the breast using the isotope sestamibi. Subjects arrive in the fasting state and have a 20 gauge intravenous catheter placed in the right antebrachium, or the left antebrachium if there is a specific question with regard to the right breast. Sestamibi is administered intravenously 4 minutes into the study followed by a 10 to 20 cc normal saline flush to ensure delivery of the isotope into the venous system, with imaging of the breast beginning 10 minutes into the study. The camera is positioned in a stationary (planar) position for each of the images. Breast imaging begins with the patient placed in a prone position on a padded surface with removable padding inserts. This allows each breast to be positioned independently through the padding in a comfortable position once the padding inserts are removed. Planar breast imaging begins with the BrQL breast (lateral view of breast in question or the right breast if neither breast is specifically suspected of having an abnormality), then the BrCL breast (lateral view of the breast contralateral to BrQL). Patients are then placed on their back for the anterior (BrAS) image of both breasts. Any areas of special concern, PO BrQ1 (posterior oblique view of first breast noted to have abnormal activity on initial views) and PO BrQ2 (posterior oblique view of the other breast if its activity is abnormal), are then imaged. The bottom panel displays the protocol for BEST imaging and is identical to the Miraluma approach except for the first 4 minutes of the study when dipyridamole (high-dose, or HDD) is infused through the intravenous catheter. The catheter is flushed with 10 to 20 cc of normal saline immediately after the HDD has been given to ensure introduction of all of the HDD into the venous system. Cardiac imaging may be initiated immediately after completion of the breast imaging if desired.*

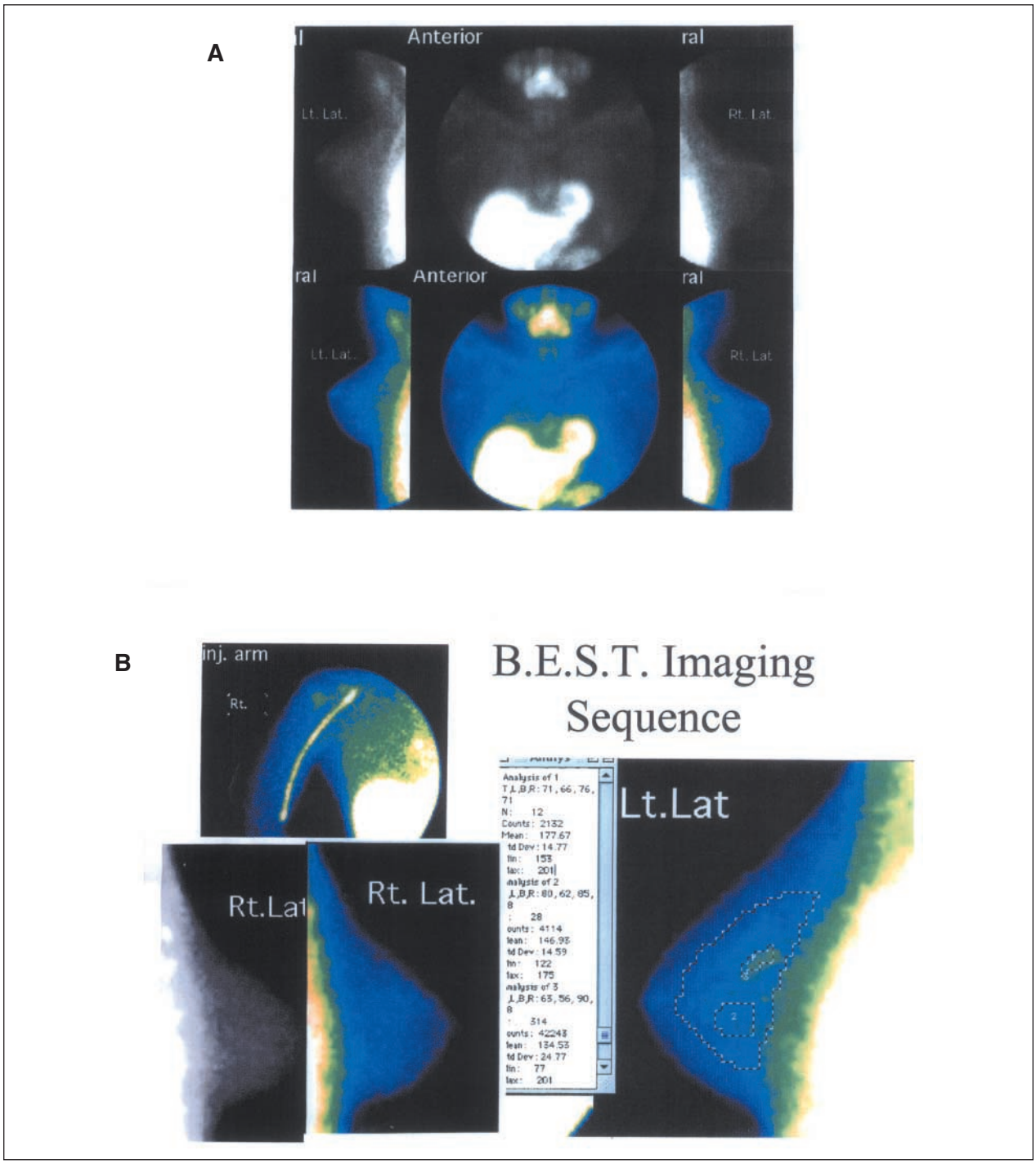

Figure 2 *(A) Examples of resting (Miraluma) and breast enhanced scintigraphy test (BEST) images in the same patient. The top row of images shows (from left to right) a lateral view of the left breast (Lt Lat), an anterior view of both breasts (BrAS), and a lateral view of the right breast (Rt Lat). These black-and-white images represent the results seen with Miraluma imaging. The bottom row of blue-green images represents the same patient following imaging with enhanced BEST imaging. The black-and-white Miraluma image was initially visually interpreted as abnormal, with the appearance of increased tracer uptake (white) in the region of the left nipple; however, the maximal count activity (MCA) revealed normal breast tissue using both approaches. (B) Sequence of BEST image presentation. Several images are displayed showing the sequence of images obtained and processed to develop the final BEST image with MCA measurement. The upper-left image reveals the isotope (sestamibi) immediately after injection into the venous system of the right arm (inj arm). Following image acquisition, a black-and-white image is displayed (Rt Lat), which is then converted into a blue-green image. Following this display of both breasts, the MCA is determined for each breast. In this case, the left breast had the greatest activity. Three regions of interest (ROIs) were measured for MCA and are displayed. Region 1 represents a smaller ROI in the upper-middle breast, with an MCA of 201. This ROI surrounds a milk duct. The second ROI was immediately below the first and had an MCA of 175. The third ROI included the entire breast, incorporating both the first and second ROIs. Consequently, the MCA of the third ROI included the first region, which had the greatest MCA of 201.*

Table 1. A Comparison of Miraluma and Breast Enhanced Scintigraphy Test (BEST) Imaging

	Normal	*Inflammatory Changes*	*Cancer*
Miraluma	107.5 ± 21.9	184.0 ± 19.2	282.5 ± 14.8
BEST	125.5 ± 31.5	228.8 ± 24.0	442.0 ± 5.7
P level	*ns*	< .05	< .005

images required to derive the final blue-green image and the MCA display of a BEST image.

Interpretation of BEST Imaging Results: MCA

Following the image reconstruction and presentation of each breast image, the region of greatest MCA was determined and quantified. This assessment of MCA was performed using computer assessment of MCA as measured and displayed on the computer monitor. All readings and determination of MCA were determined for each breast prior to any knowledge of clinical, mammographic, or pathologic information that could in any way bias the results. These procedures were performed at a recognized center of excellence for nuclear procedures under the direct supervision of a physician boarded in nuclear imaging.

Tissue Specimens

Histopathologic information was obtained for all but 58 of the individuals studied. Tissue samples were obtained through either ductoscopy, fine needle aspiration, or open biopsy and were interpreted by pathologists without knowledge of the sestamibi image results. Results were interpreted as being normal, inflammatory (evidence of leukocytes), atypia (with increasing order of cellular change progressing from hyperplasia to metaplasia/atypia to ductal carcinoma in situ), and cancer.

Statistical Analysis

The outcomes of histopathologic specimens were compared with the MCA derived from sestamibi imaging. Descriptive statistics of the MCAs were determined including mean ± standard deviation and confidence intervals (CIs) for the mean. Group comparisons were made using 2-tailed *t* tests to determine statistical differences defined as *P* values of ≤ .05. Graphic representation of the means is shown for comparison purposes, as well as raw data comparison for the histopathologic categories.

Results

Ten women were imaged during the first part of the study. One hundred ninety-five people were studied during the second part of the study. Of these 205 people, 4 were men and 201 were women. Individuals ranged in age from 29 to 88 years (51 ± 11), and the sample included 181 Caucasians, 5 Hispanics, 17 African Americans, and 2 people of Mediterranean origin. No differences in outcomes were found based on age, race, or sex.

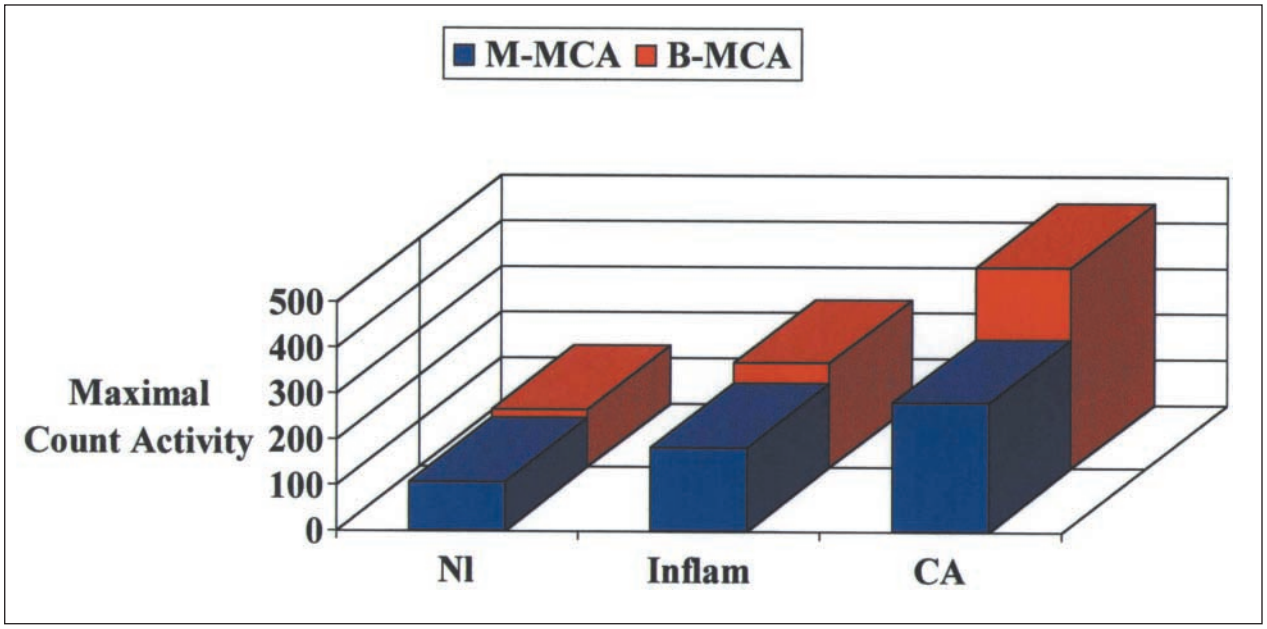

Figure 3 A comparison of maximal count activity (MCA) obtained using resting (Miraluma) and breast enhanced scintigraphy test (BEST) imaging. This bar graph represents the mean MCAs obtained for 10 people studied using both Miraluma and BEST imaging. The results of MCAs were almost identical for those with normal breast tissue. Individuals with inflammatory changes of the breast showed statistically significant differences in MCA, which were greater following BEST imaging. These differences were even greater for individuals with breast cancer. These mean standard deviation MCAs are shown in Table 1 and are statistically significant.

During the first part of the study, 10 women underwent biopsy in addition to both Miraluma and BEST imaging. Four of the women had normal breast tissue, 4 had inflammatory changes, and 2 had breast cancer. The results shown in Table 1 and Figure 3 show no difference between results obtained using either the resting (Miraluma) approach or the BEST approach in normal patients. The MCA using Miraluma was 107.5 ± 21.9 and was almost identical to that (125.5 ± 31.5) seen with BEST.

In women who had inflammatory changes, Miraluma had a statistically lower ($P < .05$) MCA of 184.0 ± 19.2 compared to that seen with BEST imaging (228.8 ± 24.0). The differences were more significant ($P < .005$) for patients with breast cancer, where BEST imaging had an MCA of 442.0 ± 5.7 and Miraluma had an MCA of 282.5 ± 14.8.

In the second part of the study, the outcomes of histopathology and MCA results using BEST imaging were compared. These results are shown in Figure 4 and reveal an exponential increase in MCA proceeding from normal to inflammatory to cancer. The MCA of patients with normal breast tissue (n = 88) ranged from 80 to 202, with an average value of 145.0 ± 29.1. The 95% CI for normal breast tissue was 139 to 151. Individuals with inflammatory changes (n = 77) had MCAs ranging from 130 to 298, with an average of 218.0 ± 40.3 and a 95% CI of 209 to 227. There were 15 individuals with cellular atypia whose MCAs ranged from 209 to 333, with an average value of 307.7 ± 29.3. The 95% CI for patients with atypia was 292 to 323. Patients with breast cancer (n = 15) had a 95% CI of 399 to 491, with an average MCA of 445.3 ± 83.3 and a range in values from 270 to 594. Breast cancers in this study ranged from 4 mm to 2 cm, with the average size being 8 to 10 mm.

When analyzed for differences between groups, there was a statistically significant difference between normal and inflammatory tissue, between inflammatory and atypia, and between atypia and cancer. In each instance, the increase was statistically significant at the $P < .001$ level. Figure 5 shows the bar graph comparisons for the 4 groups. The results demonstrate overlap between normal and inflammatory and between inflammatory and atypia, suggesting a possible transition from stage to stage. The overall appearance of cancer differed from the appearance of precancers (atypia, hyperplasia, etc.). Breast cancer was more circular, consistent with a mass effect, whereas atypia, hyperplasia, and ductal carcinoma in situ have values intermediate between inflammatory changes and cancer. These findings are consistent with increased mitochondrial activity present in these cells without increased vascularity. The appearance of ductal carcinoma in situ is typically tubular, following the ducts.

Discussion

During the first part of the study, women with normal breast tissue showed almost identical MCAs using either the resting or enhanced approaches, suggesting that the enhanced approach does not alter the delivery or uptake of sestamibi in normal breast tissue. Women with inflammatory changes showed a statistically significant increase in sestamibi when the enhanced approach was compared with the resting approach. This increase could be due to either increased vascularity present with inflammation or increased mitochondrial activity present in leukocytes when compared to normal breast tissue. Finally, the MCA for cancer following enhanced imaging was even more significant ($P < .005$) than the resting approach. This enhancement is due not only to increased vascularity but also to increased mitochondrial activity present in breast cancer.

During the second part of the study, comparisons were made between histopathologic specimens and MCA following enhanced delivery of the isotope to the breast tissue. The results in Figure 4 show an exponential increase in the uptake in sestamibi following enhancement of blood flow following HDD. This increase is most pronounced with atypia and cancer, as seen in Figure 4. This increase would be expected[28,29] in instances of increased vascularity (angiogenesis) promoted by cancers as well as the increased mitochondrial activity present in cancer cells. One cancer with an MCA of 270 clearly fell within the MCA range for "inflammatory" tissue. On further inspection, the lymph nodes were negative and the tumor had little evidence of angiogenesis. It was surgically removed, with no additional radiation therapy or chemotherapy recommended to the patient by her oncology team.

The importance of immunologic responses to disease in the human body is present in both heart disease[30] and cancer. The role in tumors includes natural killer cells, cytokines, interleukins, and so on. Just as patients do not go from having zero heart disease to needing a bypass operation, there is logically a progression from normal breast tissue to breast cancer as a variety of factors influence breast tissue. Enhancement of the delivery of sestamibi to breast tissue permits not only a distinction of normal versus breast cancer but also a distinction between normal, regions of inflammatory changes of the breast, regions of cellular atypia, and breast cancer. Although not all regions of inflammatory changes are destined to become cancer, these regions may represent regions at greater risk of becoming a cancer, subsequently needing closer

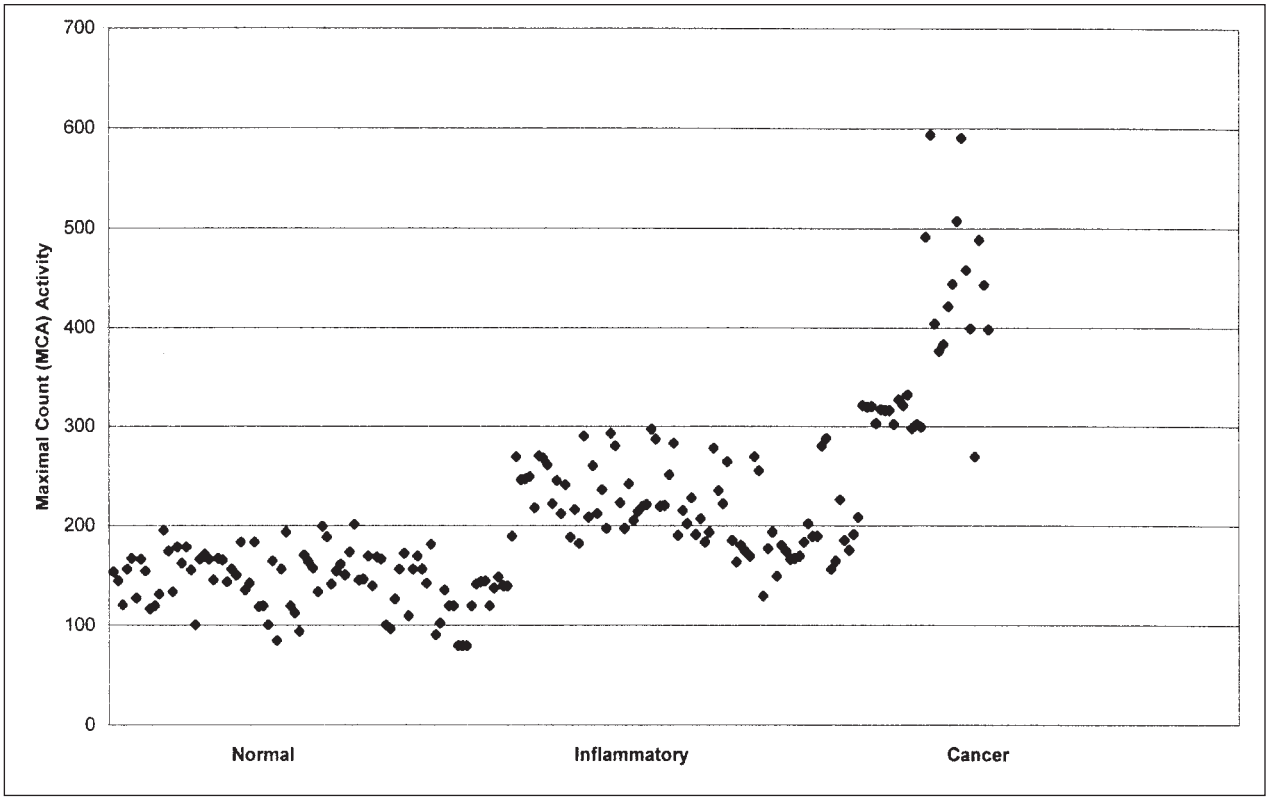

Figure 4 Graphic representation of the results of maximal count activity (MCA) as seen in normal, inflammatory tissue, and breast cancer. MCA is plotted and displayed showing a grouping of results revealing differences between normal, inflammatory tissues, and breast cancer. These differences displayed an exponential increase in MCA progressing from normal to breast cancer.

monitoring to determine whether they are progressing to the development of a cancer. Clearly, the sooner a cancer is detected, the greater is the likelihood of successful treatment.

The appearance of lesions seen on BEST imaging demonstrated differences in the appearance of cancers and pre-cancers. For example, ductal carcinoma in situ appeared tubular, following the path of the milk ducts, whereas breast cancer appears spherical. This is entirely consistent with what should be expected. Pre-cancers should demonstrate cellular changes that still abide by some normal cellular

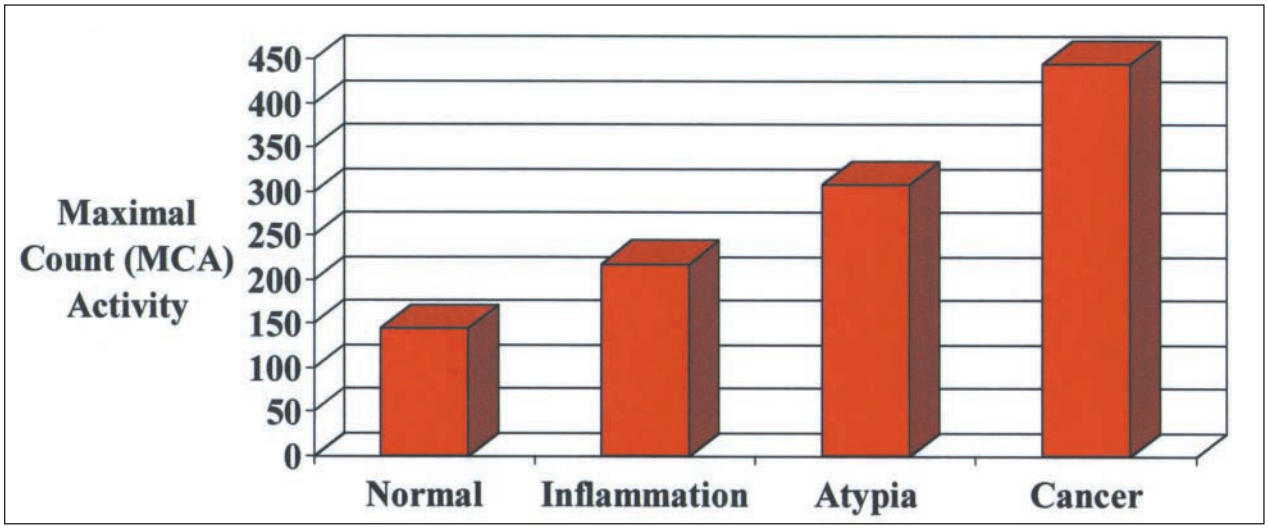

Figure 5 Differences in maximal count activity (MCA) in individuals with normal, inflammatory, atypia, and cancerous breast tissue. The raw data (Figure 4) were analyzed following histopathologic results. The mean MCAs for each of 4 groups (normal, inflammatory, atypia, and cancer) are displayed. These mean standard deviation MCAs are shown in Table 2 and are statistically significant.

Table 2. Differentiation of Tissue Based on Breast Enhanced Scintigraphy Test (BEST) Maximal Count Activity (MCA) Results

	Normal	*Inflammatory Changes*	*Atypia/ Metaplasia*	*Cancer*
MCA	145.0 ± 29.1	218.0 ± 40.3	307.7 ± 29.3	445.3 ± 83.3

mechanisms (eg, contact inhibition), resulting in linear growth along the milk ducts. However, once these cells have changed further, they no longer obey contact inhibition and subsequently grow into surrounding tissue, producing a spherical appearance in the same way they behave in the laboratory. These changes in appearance therefore can be used to distinguish early cancers/pre-cancers from the next stage of infiltrating cancer.

Conclusion

The detection of breast cancer is based on the ability to find either an anatomic or a physiologic abnormality. Prior efforts to detect breast cancers physiologically using sestamibi have employed a resting (Miraluma) approach. Enhancement of blood flow to the heart using HDD has proven useful in unmasking earlier heart disease through augmentation of regional blood flow differences and now appears to be useful in the diagnosis of breast cancer and breast disease. The uptake of sestamibi is dependent on both the delivery of the isotope through the vascular bed and the presence of mitochondrial activity once the isotope has been delivered. Breast cancers, like other cancers, theoretically have increased vascularity resulting from angiogenic activity, which presumably increases blood supply to the cancer and provides nutrients for growth and survival. Cancers and inflammatory tissue have greater mitochondrial activity than normal tissue, which has greater activity than injured or necrotic tissue.

Based on the assumption that breast cancer should have increased vascularity, which could be affected by the vasodilatory effects of dipyridamole (HDD), and greater mitochondrial activity, which could be further detected once increased delivery of isotope is provided through enhanced blood flow, the first part of this study was designed to determine whether such differences could be detected, and they were. In the first part of this study, no difference between the nonenhanced (Miraluma) and enhanced (BEST) delivery of the isotope (sestamibi) was demonstrated in normal breast tissue, where no increase in vascularity or mitochondrial activity was present. When inflammatory changes were present, there was some increase in both vascularity and mitochondrial (leukocytes, fibroblasts, etc.) activity. Under these circumstances, there was a statistically significant increase in isotope activity as measured by MCA following the enhanced delivery of sestamibi using BEST. This increase was more noticeable when cancer was present, with even greater mitochondrial activity and angiogenesis. The MCA was less significant when vascularity and mitochondrial activity were less pronounced.

In the second part of this study, a larger population of individuals was studied. Their histopathologic findings were compared to results obtained with BEST imaging. The findings continued to demonstrate differences based on vascularity and mitochondrial activity and demonstrated the ability to distinguish across a continuum of breast tissue changes ranging from normal to inflammatory to atypia to cancer. These distinctions support a hypothesis of a transition from normal breast tissue to breast cancer and offer a method for distinguishing between changes in breast tissue and possible earlier detection and monitoring of breast cancer.

References

1. Khalkhali I, Cutrone JA, Mena IG, et al. Scintimammography: the complementary role of Tc-99m sestamibi prone breast imaging for the diagnosis of breast carcinoma. *Radiology.* 1995;196:421-426.
2. Khalkhali I, Villanueva-Meyer J, Edell SL, et al. Diagnostic accuracy of 99mTc-sestamibi breast imaging: multicenter trial results. *J Nucl Med.* 2000;41:1973-1979.
3. Carvalho PA, Chiu ML, Kronauge JF, et al. Subcellular distribution and analysis of technetium-99m-MIBI in isolated perfused rat hearts. *J Nucl Med.* 1992;33:1516-1522.
4. Piwnica-Worms D, Kronauge JF, Chiu ML. Uptake and retention of hexakis (2-methoxyisobutyl isonitrile) technetium (I) in cultured chick myocardial cells: mitochondrial and plasma membrane potential dependence. *Circulation.* 1990;82:1826-1838.
5. Vanoli C, Antronaco R, Giovanella L, Ceriani L, Sessa F, Fugazzola C. 99mTc-MIBI characterization of breast microcalcifications: correlations with scintigraphic and histopathologic findings. *Radiol Med.* 1999;98:19-25.
6. Benard F, Lefebvre B, Beuvon F, Langlois MF, Bisson G. Rapid washout of technetium-99m-MIBI from a large parathyroid adenoma. *J Nucl Med.* 1995;36:241-243.
7. Arbab AS, Koizumi K, Hemmi A, et al. Tc-99m-MIBI scintigraphy for detecting parathyroid adenoma and hyperplasia. *Ann Nucl Med.* 1997;11:45-49.
8. Chiu ML, Kronauge JF, Piwnica-Worms D. Effect of mitochondrial and plasma membrane potentials on accumulation of hexakis (2-methoxyisobutylisonitrile) technetium (I) in cultured mouse fibroblasts. *J Nucl Med.* 1990;31:1646-1653.
9. Backus M, Piwnica-Worms D, Hockett D, et al. Microprobe analysis of Tc-MIBI in heart cells: calculation of mitochondrial membrane potential. *Am J Physiol.* 1993;265:C178-C187.
10. Scopinaro F, De Vincentis G, Pani R, et al. 99Tcm-MIBI uptake in green plants. *Nucl Med Commun.* 1994;15:905-915.
11. Arbab AS, Koizumi K, Toyama K, Araki T. Uptake of technetium-99m-tetrofosmin, technetium-99m-MIBI and thallium-201 in tumor cell lines. *J Nucl Med.* 1996;37:1551-1556.
12. Crane P, Laliberte R, Heminway S, Thoolen M, Orlandi C. Effect of mitochondrial viability and metabolism on

technetium-99m-sestamibi myocardial retention. *Eur J Nucl Med*. 1993;20:20-25.

13. Piwnica-Worms DP, Kronauge JF, LeFurgey A, et al. Mitochondrial localization and characterization of 99Tc-SESTAMIBI in heart cells by electron probe X-ray microanalysis and 99Tc-NMR spectroscopy. *Magn Reson Imaging*. 1994;12:641-652.
14. Pach J, Hubalewska-Hola A, Szybinski Z, Pach D. New possibilities in scintigraphy detection of carbon monoxide cardiotoxicity. *Przegl Lek*. 2001;58:182-184.
15. Piwnica-Worms D, Chiu ML, Kronauge JF. Detection of adriamycin-induced cardiotoxicity in cultured heart cells with technetium 99m-SESTAMIBI. *Cancer Chemother Pharmacol*. 1993;32:385-391.
16. Gunningham SP, Currie MJ, Han C, et al. VEGF-B expression in human primary breast cancers is associated with lymph node metastasis but not angiogenesis. *J Pathol*. 2001;193:325-332.
17. Pepper MS. Extracellular proteolysis and angiogenesis. *Thromb Haemost*. 2001;86:346-355.
18. Zhong S, Zhang Z, Li S. Significance of vascular endothelial growth factor expression in colorectal cancer. *Zhonghua Nei Ke Za Zhi*. 2001;40:514-516.
19. Fleming RM. Atherosclerosis: understanding the relationship between coronary artery disease and stenosis flow reserve. In: Chang JC, ed. *Textbook of Angiology*. New York, NY: Springer-Verlag; 1999:381-387.
20. Fleming RM. Nuclear cardiology: its role in the detection and management of coronary artery disease. In: Chang JC, ed. *Textbook of Angiology*. New York, NY: Springer-Verlag; 1999:397-406.
21. Fleming RM, Boyd L, Forster M. Angina is caused by regional blood flow differences—proof of a physiologic (not anatomic) narrowing. Paper presented at: Joint Session of the European Society–American College of Cardiology, ACC 49th Annual Scientific Sessions; March 12, 2000; Anaheim, CA.
22. Fleming RM. Regional blood flow differences induced by high dose dipyridamole explain etiology of angina. Paper presented at: 3rd International College of Coronary Artery Disease From Prevention to Intervention; October 4, 2000; Lyon, France.
23. Fleming RM, Boyd LB, Kubovy C. Myocardial perfusion imaging using high dose dipyridamole defines angina: the difference between coronary artery disease (CAD) and coronary lumen disease (CLD). Paper presented at: 48th Annual Scientific Session of the Society of Nuclear Medicine; June 27, 2001; Toronto, Ontario, Canada.
24. Fleming RM. Coronary artery disease is more than just coronary lumen disease. *Am J Cardiol*. 2001;88:599-600.
25 Fleming RM, Rose CH, Feldmann KM. Comparing a high-dose dipyridamole SPECT imaging protocol with dobutamine and exercise stress testing protocols. *Angiology*. 1995;46:547-556.
26. Holdright DR, Lindsay DC, Clarke D, Fox K, Poole-Wilson PA, Collins P. Coronary flow reserve in patients with chest pain and normal coronary arteries. *Br Heart J*. 1993;70:513-519.
27. Fleming RM, Dooley WC, Boyd LB, Kubovy C. Breast enhanced scintigraphy testing (BEST)—increased accuracy in detecting breast cancer accomplished by combining breast and cardiac imaging. Paper presented at: 48th Annual Scientific Session of the Society of Nuclear Medicine; June 26, 2001; Toronto, Ontario, Canada.
28. Folkman J, Merler E, Abernathy C, Williams G. Isolation of a tumor factor responsible for angiogenesis. *J Exp Med*. 1971; 133:275-288.
29. Stewart RJ, Panigraphy D, Flynn E, Folkman J. Vascular endothelial growth factor expression and tumor angiogenesis are regulated by androgens in hormone responsive human prostate carcinoma: evidence for androgen dependent destabilization of vascular endothelial growth factor transcripts. *J Urol*. 2001;165:688-693.
30. Fleming RM. The pathogenesis of vascular disease. In: Chang JC, ed. *Textbook of Angiology*. New York, NY: Springer-Verlag; 1999:787-798.

Dr. Keith Block has withdrawn himself from the process of review and acceptance of this article, due to his exploration of potential commercial applications of the BEST procedure.